Biomaterials Science

PAPER

View Article Online
View Journal | View Issue

Development of microbial resistant Carbopol nanocomposite hydrogels *via* a green process

Cite this: *Biomater. Sci.*, 2014, **2**, 257

Kokkarachedu Varaprasad,*[a,b] G. Siva Mohan Reddy,[b] J. Jayaramudu,[b] Rotimi Sadiku,[b] Koduri Ramam[a] and S. Sinha Ray[c]

Received 29th July 2013,
Accepted 16th September 2013

DOI: 10.1039/c3bm60185d

www.rsc.org/biomaterialsscience

The present scientific research resulted in the development of novel microbial resistant inorganic nanocomposite hydrogels, which can be used as antibacterial agents. They are promising candidates for advanced antimicrobial applications in the field of biomedical science. Novel inorganic nanocomposite hydrogels were developed from Carbopol® 980 NF and acrylamide. Dual-metallic (Ag^0–Au^0) nanoparticles were prepared (*via* a green process) by the nucleation of silver and gold salts with mint leaf extract to form a hydrogel network. The Carbopol nanocomposite hydrogels contain (Ag^0–Au^0) nanoparticles ~5 ± 3 nm in size, which was confirmed by transmission electron microscopy. The developed hydrogels were characterized using Fourier transform infrared (FTIR) spectroscopy, thermo-gravimetric analysis (TGA), scanning electron microscopy-energy dispersive spectroscopy (SEM-EDS) and transmission electron microscopy (TEM). The pure and inorganic nanocomposite hydrogels developed were tested against *Bacillus* and *E. coli*, for their antibacterial properties. The results indicate that the inorganic nanocomposites show significantly greater antimicrobial activity than the pure hydrogels. Therefore, novel microbial resistant Carbopol nanocomposite hydrogels can be used as potential candidates for antibacterial applications.

1. Introduction

In the last decade, there has been an increase in the development of dual-metallic (inorganic) polymer materials with well structured morphology because their unique optical, electronic, magnetic and catalytic characteristics are of general interest in engineering, medicine and technical applications.[1,2] In the medical field, inorganic hydrogels are increasingly employed as antibacterial agents for clinical use, due to their numerous and highly beneficial properties.[3–6] Principally, the 3D (three-dimensional) microstructures of hydrogels can easily stabilize inorganic and organic materials without agglomeration and they are able to release the particles in an aqueous medium (expected pH medium); this characteristic makes them attractive in the biomedical and biotechnological fields.[7,8] Recently, Varaprasad *et al.*[9–11] fabricated organic and inorganic nanostructured materials for applications in drug delivery and the inactivation of bacteria. Murali *et al.*[12] reported on nanostructured hydrogels and their uses in science. Jayaramudu and his coworkers[13] reported on biodegradable hydrogels for the inactivation of bacteria.

So far, many researchers have synthesized inorganic nanocomposite hydrogels using a physical and chemical cross-linking method,[14] whereby toxic chemicals, which are harmful to living systems, were used for the reduction of the inorganic particles.[13] To solve this problem, researchers have introduced 'green processes'.[13] In a few of the green processes researchers have used plant leaf extracts as reducing agents for inorganic nanoparticles, since they (leaf extracts) are cost-effective and also require ambient conditions for the reduction reaction.[15] The green reduction process of inorganic ions to inorganic nanoparticles can be facilitated with a high degree of efficiency in a hydrogel network and by controlling the inorganic salts, the formation of the nanoparticles and the way in which the nanoparticles embed in the hydrogel networks was controlled.[16] This special character of hydrogels mainly depends on the hydrogels' composition[4] and hence by varying their composition; hydrogels were fabricated to be employed in biomedical applications.[17] Varaprasad *et al.*[4] have reported the fabrication of various types of hydrogels by varying their compositions.

The present work explores the development of microbial resistant Carbopol nanocomposite hydrogels from Carbopol®

[a]*Departamento de Ingeniería de Materiales-DIMAT, Facultad de Ingeniería Universidad de Concepción, Concepción, Chile. E-mail: varmaindian@gmail.com, kvaraprasad@udec.cl*
[b]*Department of Polymer Technology, Tshwane University of Technology, CSIR Campus, Building 14D, Private Bag X025, Lynwood Ridge 0040, Pretoria, South Africa*
[c]*DST/CSIR Nanotechnology Innovation Centre, National Centre for Nano-Structured, Materials, Council for Scientific and Industrial Research, Pretoria 0001, South Africa*

980 NF (C980) and acrylamide (AM) *via* a green process. C980 is a water soluble vinyl polymer, which is a non-toxic and non-irritant material with no evidence of its hypersensitivity in humans when used topically.[18] C980 and its derivative products have a variety of uses in biomedical fields, such as for: vaginal drug delivery, anti-cancer and anti-HIV-1 applications.[19–21] Due to its characteristics that are suitable for biomedical applications, C980 was selected for the preparation of the inorganic core–shell nanocomposite hydrogels. In this regard, we have utilized (as a natural reducing agent) mint leaf extract, which is a highly biologically active compound.[22] Mint leaf is naturally-occurring, non-toxic and is an excellent bio-active agent for humans (wound healing properties).[23] Structural, thermal and morphological studies of the hydrogels and their corresponding inorganic core–shell nanocomposite hydrogels were carried out by using Fourier transform infrared (FTIR) spectroscopy. The content and distribution of the dual nanoparticles in Poly(Carbopol® 980 NF-Acrylamide) P(C980-AM) hydrogels were determined by thermogravimetric analysis (TGA), scanning electron microscopy-energy dispersive spectroscopy (SEM-EDS) and transmission electron microscopy (TEM). The effect of dual nanoparticles on the antibacterial activity of the P(C980-AM) hydrogels was studied. Herein, a study on designing P(C980-AM) core–shell inorganic nanocomposite hydrogels for their significant antibacterial applications is presented.

2. Experimental

2.1. Materials

Carbopol® 980 NF (Lubrizol, batch number: 0100648897) was obtained as a gift sample from Lubrizol Advanced Materials Europe. Acrylamide (AM), *N*,*N*^{1}-methylenebisacrylamide (MBA), ammonium persulphate (APS), silver nitrate ($AgNO_3$) and gold chloride ($H{\cdot}AuCl_4{\cdot}xH_2O$) were purchased from SD Fine Chemicals (Mumbai, India). Distilled water was used for all the polymerizations and solution preparations.

2.2. Preparation of the leaf extract

Leaf extracts were prepared by a green process, using the standard procedure described by Jayaramudu *et al.*[15] Mint leaves were collected and thoroughly washed with distilled water. Mint leaf broth was prepared by placing 25 g of thoroughly washed and finely cut leaves in a 1000 ml Erlenmeyer flask with 500 ml of sterile distilled water. The solution was heated at 100 °C for 2 min in order to extract the contents of the leaves, and filtered through a 0.45 μm PVDF Millex Filter using a 50 ml syringe. The extracted leaf solutions were stored at 4 °C.

2.3. Synthesis of the hydrogel

AM (14.06 mM) and various ratios (0.05–0.15 g) of C980 were dissolved in 3 ml of distilled water by stirring at 300 rpm for 2 h at ambient temperature. To this solution, 1 ml (0.64 mM) of MBA and 1 ml (2.191 mM) of APS were added. After the addition of the reactants the temperature of the system was raised to 50 °C for 25 min. Free-radical polymerization was carried out at ambient temperature for 8 h. After completion of the reaction, the hydrogel was immersed in distilled water at ambient temperature for 24 h in order to remove the unreacted materials present in the hydrogel network. Finally, the hydrogel was dried at ambient temperature for 48 h. Similarly, other hydrogels were prepared using the procedure described above.

2.4. Synthesis of the core–shell inorganic nanocomposite hydrogel

To prepare the bi-metallic nanocomposite hydrogel, the required amounts of dried hydrogel were immersed in a large amount of distilled water for 2 days in order to swell it to its full extent. The swollen hydrogel was transferred into a 250 ml beaker and immersed in 20 ml of 5 mM $AgNO_3$ and 10 ml of $H{\cdot}AuCl_4{\cdot}xH_2O$ (5 mM) aqueous solutions in order to allow equilibration for 24 h. The hydrogel was removed and transferred to a cold mint leaf extract solution, for 4 h for the reduction of the metal ions. The hydrogel nanocomposite was dried at ambient temperature. It was powdered and used for characterization. Table 1 illustrates the various components used in the preparation of P(C980-AM) hydrogels.

2.5. Characterization

A FTIR spectrophotometer was used to study the transmission of the hydrogel pattern and dual-metallic nanoparticle patterns in the hydrogel networks. The hydrogels and the dual-metallic nanoparticle-embedded P(C980-AM) hydrogels were completely dried in an oven (Baheti Enterprises, Hyderabad, India) at 60 °C for 6 h before the respective FTIR experiments were carried out. Samples were examined between 500 and 4000 cm^{-1} on a Bruker IFS 66 V FTIR spectrometer (Ettlingen, Germany), using the KBr disk method. Scanning electron microscopy-energy dispersive spectroscopy (SEM-EDS) analyses of the plain P(C980-AM) hydrogel and dual-metallic nanoparticle impregnated P(C980-AM) hydrogels were performed using a JEOL JEM-7500F (Tokyo, Japan), operated at an accelerating voltage of 2 kV. All samples were carbon-coated, prior to examination on a field emission scanning electron microscope. A transmission electron microscope (TEM) (JEM-1200EX, JEOL, Tokyo, Japan) was used for morphological observations. A TEM sample was prepared by dispersing two to three drops of the finely ground P(C980-AM) dual-metallic nanocomposite (1 mg ml^{-1}) solution on a 3 mm copper grid and dried at

Table 1 Feed composition for the preparation of P(C980-AM) hydrogels

Hydrogel code	AM (mM)	C980 (g)	MBA (mM)	APS (mM)
P(C980-AM) 0	8.837	0.0	0.648	2.191
P(C980-AM) 1	8.837	0.05	0.648	2.191
P(C980-AM) 2	8.837	0.10	0.648	2.191
P(C980-AM) 3	8.837	0.15	0.648	2.191

ambient temperature after removing the excess solution using filter paper.

The swelling ratios of the hydrogel samples were measured at ambient temperature, using a gravimetric method.[24,25] The dried hydrogels were immersed in a 50 ml beaker containing double distilled water until their weights became constant. The hydrogels were then removed from water and their surfaces were blotted with filter paper before being weighed. Furthermore, swollen hydrogels were treated with a dual-metallic aqueous solution and subsequently with mint solution; a green process, as explained in the experimental section. The swelling ratio or swelling capacity ($S_{g/g}$) of the hydrogel developed or the respective nanocomposite was calculated using eqn (1):

$$\text{Swelling ratio } (S_{g/g}) = [W_s - W_d]/W_d \quad (1)$$

where W_s and W_d denote the weights of the swollen hydrogel at equilibrium and the weight of the dry hydrogel, respectively. The data provided is an average of 3 individual sample readings.

2.6 Antibacterial activity

The antibacterial activity of the inorganic nanocomposite P(C980-AM) hydrogels, was investigated using the disc method, according the standard procedure described elsewhere.[26,27] Nutrient agar medium was prepared by mixing peptone (5.0 g), beef extract (3.0 g) and sodium chloride (NaCl) (5.0 g) in distilled water (1000 ml) and the pH was adjusted to 7.0. Finally, agar (15.0 g) was added to the solution. The agar medium was sterilized in a conical flask at a pressure of 6.8 kg (15 lbs) for 30 min. This medium was transferred into sterilized petri dishes in a laminar air flow chamber (Microfilt Laminar Flow Ultra Clean Air Unit, India, Mumbai). After solidification of the media, bacteria (*Bacillus*, *E. coli*) (50 μl) were spread on the solid surface of the media for the culture experiment. Onto this inoculated petri dish, one drop of the gel solutions (20 mg per 10 ml distilled water) was added using a 10 μl tip and the plates were incubated for 48 h at 37 °C.

3. Results and discussion

The present work focuses on investigating the potential of novel Carbopol nanocomposite hydrogels (core–shell or dual-metallic nanoparticles) for the inactivation of bacteria and further possible applications. Core–shell nanoparticles in hydrogel networks were successfully prepared by using mint leaf *via* a green process, as shown in Scheme 1. Carbopol (C980) was employed as the stabilizer for the development of the P(C980-AM) hydrogels. The results of the characterization of the prepared C980 inorganic nanocomposite hydrogels can be seen in Fig. 1–6. These analyses demonstrate that highly exfoliated core–shell nanocomposite hydrogels have been successfully prepared.

The core–shell nanoparticle formation depends principally on the swelling behaviour of hydrogels. The results in Fig. 1 show that the values of the swelling characteristics were influenced by the hydrogel concentration; with an increase in the C980 concentration resulting in increases in the swelling ratio values of the conventional and dual-metallic nanocomposite hydrogels. This is due to the hydrophilic nature of C980. However, the formed dual-metallic nanocomposite hydrogels have higher swelling ratios, when compared to the conventional P(C980-AM) hydrogels. The reason being that when Ag^{+}–Au^{3+} ion-loaded hydrogels were treated with mint extract, the addition of many Ag^{+}–Au^{3+} ions led to the formation of the nanoparticles within the hydrogel, which expanded the hydrogel networks and promoted a higher water uptake

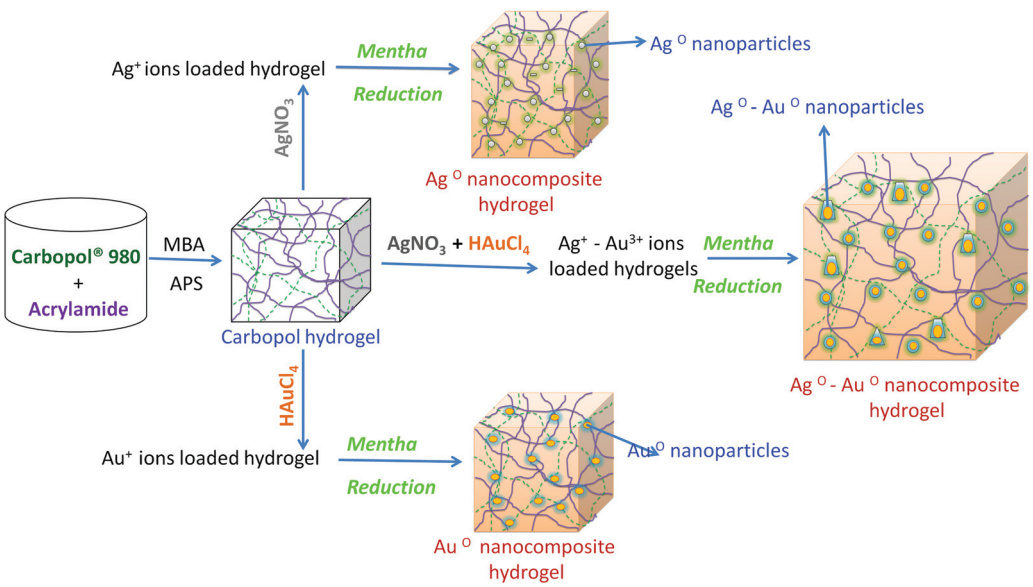

Scheme 1 Schematic diagram for the formation of P(C980-AM) + Ag^0 + Au^0 nanocomposite hydrogels.

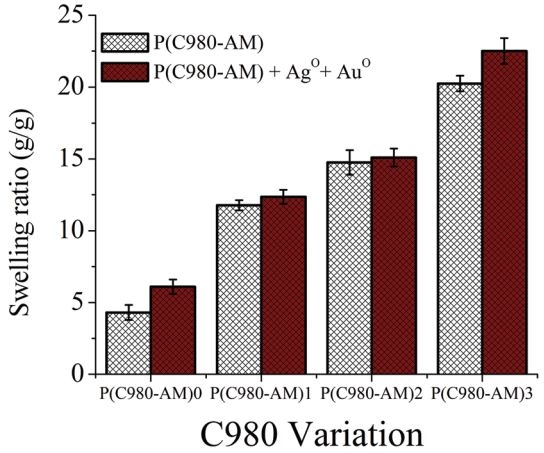

Fig. 1 Swelling behavior of hydrogels with different concentrations of C980 and dual-metallic nanocomposite hydrogels.

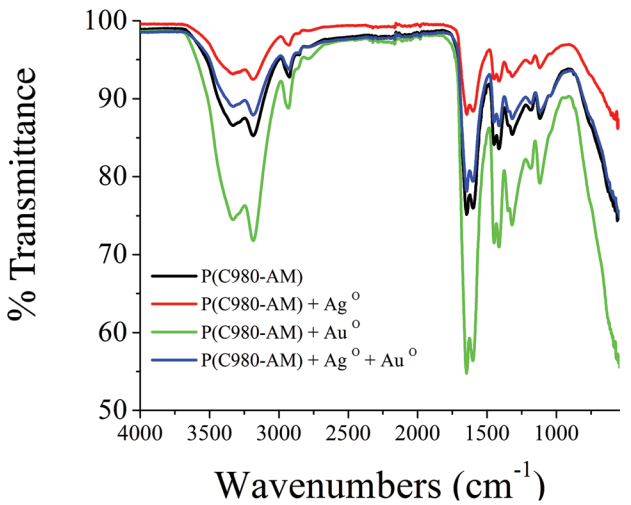

Fig. 2 FTIR spectra of pure P(C980-AM)3 hydrogel, P(C980-AM)3 + Ag^0, P(C980-AM)3 + Au^0 and P(C980-AM)3 + Ag^0 + Au^0 nanocomposite hydrogels.

capacity. This interesting phenomenon could play a significant role in biomedical applications, particularly in wound care applications.

Fig. 2 shows the FTIR spectra of pure [P(C980-AM)], single metallic [P(C980-AM) + Ag^0, P(C980-AM) + Au^0] and dual metallic [P(C980-AM) + Ag^0 + Au^0] nanocomposite hydrogels. The spectrum of the P(C980-AM) hydrogel shows a broad absorption band at 3338 cm^{-1} that is related to the –NH asymmetric and –OH symmetric stretching vibrations, the bands at 2928 cm^{-1} are attributed to stretching vibrations of the $-CH_3$ unit and the absorption band at 1646 cm^{-1} is from the carbonyl groups of the P(C980-AM) hydrogel. The other main characteristic peaks of C980 at 1184 and 1121 cm^{-1} were assigned to the carbonyl group.[28] However, these peaks shifted in the case of the single metallic [P(C980-AM) + Ag^0, P(C980-AM) + Au^0] and dual metallic nanocomposite hydrogels [P(C980-AM) + Ag^0 + Au^0]. Table 2 illustrates the important peaks observed for the single metallic [P(C980-AM) + Ag^0, P(C980-AM) + Au^0] and dual metallic nanocomposite hydrogels [P(C980-AM) + Ag^0 + Au^0]. Overall, the shifting of the peaks confirms the formation of core–shells nanoparticles with Carbopol, which provides significant stabilization for the core–shells nanoparticles formed.

The structure and elemental composition of the core–shell nanoparticles were investigated by means of SEM-EDS. The hydrogel morphology (stabilization of core–shells) is obviously dependent on the C980 content in the hydrogels (Fig. 3). Fig. 3a shows that the dual-metallic loaded nanocomposite hydrogel [P(C980-AM)1] has fewer nanoparticles in its structure, whereas from Fig. 3b and c it is obvious that a huge quantity of dual-metallic nanoparticles was dispersed on the [P(C980-AM)3] hydrogel surface. This is due to the C980 concentration in the hydrogel network, which considerably stabilizes the core–shell nanoparticles. Furthermore, EDS was employed to confirm the presence of core–shell nanoparticles in the P(C980-AM) hydrogel. The EDS spectra of the dual-metallic loaded nanocomposite hydrogels were then investigated. The spectrum of the dual-inorganic nanocomposite hydrogels (Fig. 3d) shows clearly the peaks of Au^0 and Ag^0. The intensity of the Au^0 and Ag^0 peaks are proportional to the metal concentration in the hydrogel composites. Therefore, the existence of core–shell nanoparticles on the hydrogel is confirmed by the EDS spectra. The C980 in the networks is used to stabilize the core–shell nanoparticles formed in the hydrogel networks.

In order to analyze the structure and size of the core–shell nanoparticles, transmission electron microscopy (TEM) measurements are also performed. As shown in Fig. 4, the different images of the particles indicate the formation of core–shell (Ag^0–Au^0) nanoparticles, which have different shapes and their average size is ~5 ± 3 nm. It is evident that Ag^0 nanoparticles are highly stabilized by using C980 in the hydrogel network. These results are mainly due to the strong interaction between the Ag^0–Au^0 nanoparticles and P(C980-AM) hydrogels.

Furthermore, thermogravimetric analysis was used to study the formation of core–shell nanoparticles and the thermal stability of the different hydrogels. As shown in Fig. 5, the thermal decomposition of pure [P(C980-AM)] and single metallic nanocomposite hydrogels [P(C980-AM) + Ag^0 and P(C980-AM) + Au^0], occurred at 625 °C with a significant mass loss of 99.81%, 98.12%, 96.59%, respectively. For the dual metallic nanocomposite hydrogel [P(C980-AM) + Ag^0 + Au^0], a comparatively very low mass loss (94%) was observed at 625 °C, which was due to the partial decomposition of the Ag^0 and Au^0 nanoparticles. Moreover, according to the TGA results, the dual metallic nanocomposite hydrogels [P(C980-AM) + Ag^0 + Au^0] showed a higher thermal stability when compared with the other hydrogels.

Inorganic nanoparticles inherently possess bacteria-killing properties, but by modifying the inorganic nanoparticles these properties can be improved. Recently in the biomedical field, a synthesis of much smaller core–shell nanoparticles by a green process was developed to enhance the inactivation of bacteria in wounds.

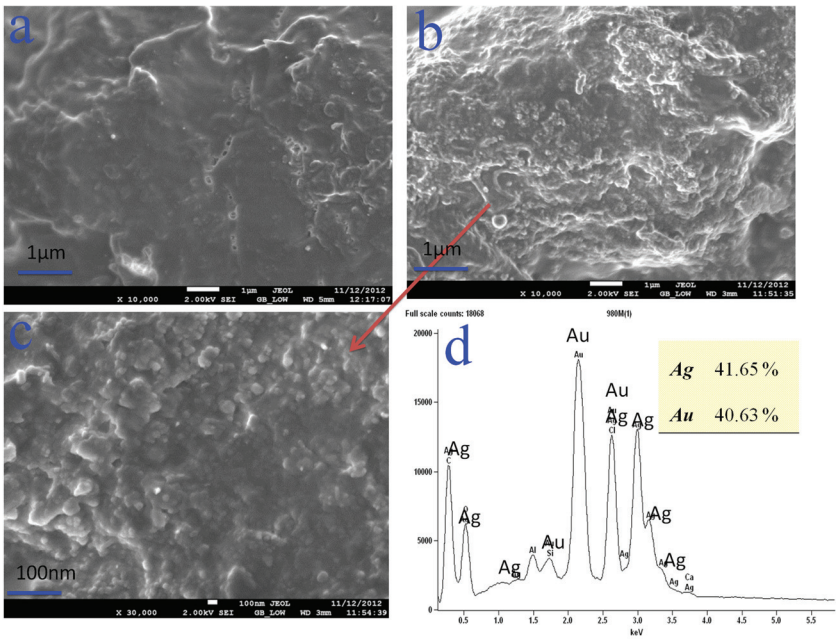

Fig. 3 SEM images of: (a) P(C980-AM)1 + Ag^0 + Au^0, (b, c) P(C980-AM)3 + Ag^0 + Au^0 nanocomposite hydrogels, EDS images of: (d) P(C980-AM)3 + Ag^0 + Au^0 nanocomposite hydrogel.

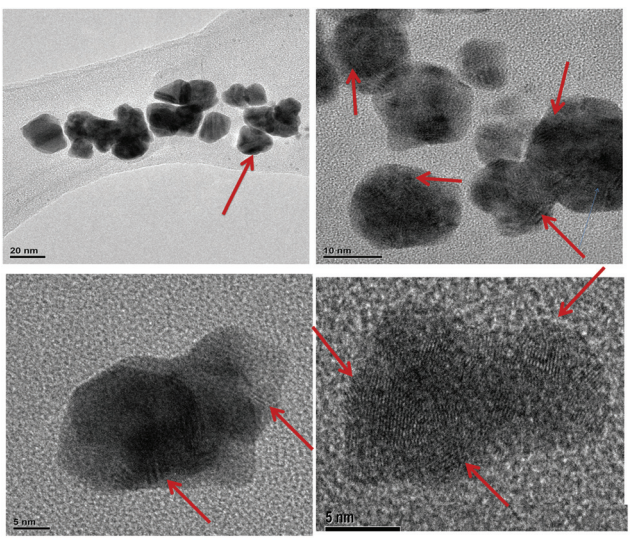

Fig. 4 TEM images of P(C980-AM)3 + Ag^0 + Au^0 nanocomposite hydrogel.

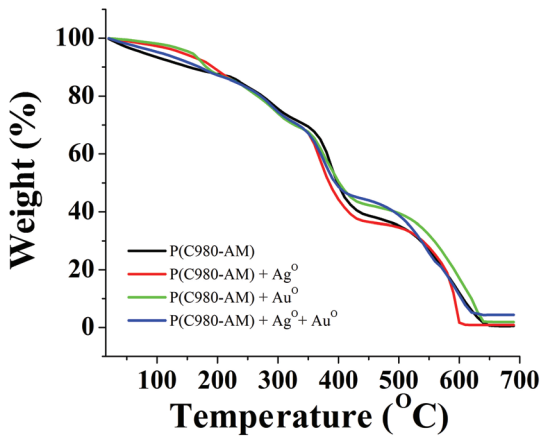

Fig. 5 TGA curves of: pure P(C980-AM)3 and P(C980-AM)3 + Ag^0, P(C980-AM)3 + Au^0 and P(C980-AM)3 + Ag^0 + Au^0 nanocomposite hydrogels.

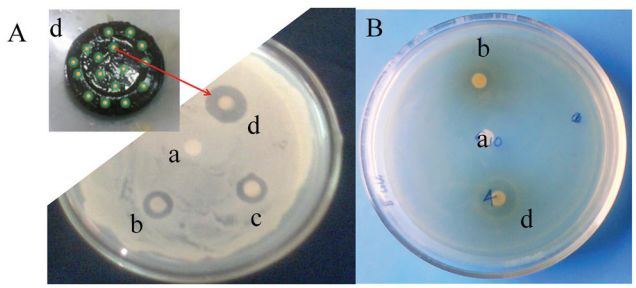

Fig. 6 Antibacterial activity. A: (a) plain P(C980-AM)3, (b) P(C980-AM)3 + Ag^0, (c) P(C980-AM)3 + Au^0 and (d) P(C980-AM)3 + Ag^0 + Au^0 nanocomposite hydrogels on *Bacillus*. B: (a) plain P(C980-AM)3, (b) P(C980-AM)3 + Ag^0 and (d) P(C980-AM)3 + Ag^0 + Au^0 nanocomposite hydrogels on *E. coli*.

The mechanism of the inhibitory effect of AgNPs towards the growth of microorganisms is not clear.[29] However, among the various possible mechanisms proposed,[29] the 'Inhibition by formation of *pits*' mechanism was considered at this point. The initial contact of the core–shell inorganic hydrogels with the microbes allows the core–shells to interact with the cell wall of the microbe membrane to form pits. These pits cause polymer molecules and membrane proteins of the bacteria to leak, leading to microbial death.[30] Fig. 6A,B support this conclusion. The dual nanoparticles enter into the bacteria cell more effectively, causing damage to the nuclei and resulting in

Table 2 Fourier transform infrared spectral data of the C980 based hydrogels

Hydrogel code	FTIR bands (cm^{-1})
P(C980-AM)	3338.3, 2928.0, 1646.5, 1415.1, 1184.2, 1121.3
P(C980-AM) + Ag^0	3331.6, 2925.5, 1643.3, 1415.3, 1184.6, 1121.8
P(C980-AM) + Au^0	3340.6, 2932.6, 1650.2, 1416.2, 1184.2, 1122.5
P(C980-AM) + Ag^0 + Au^0	3333.9, 2923.6, 1646.4, 1418.1, 1171.6, 1117.0

faster bacterial death. The antimicrobial efficacy of the bimetallic hydrogels developed from core–shell nanoparticles was examined against *Bacillus* and *E. coli* model bacteria. The effects of the P(C980-AM)], P(C980-AM) + Ag^0, P(C980-AM) + Au^0 and P(C980-AM) + Ag^0 + Au^0 hydrogels on bacteria are shown in Fig. 6. The diameters of the inhibition zones for the P(C980-AM) + Ag^0 + Au^0 hydrogel (Fig. 6Ad 1.85 cm, Fig. 6Bd 1.81 cm) are larger than those for the P(C980-AM) + Ag^0, P(C980-AM) + Au^0 hydrogels (Fig. 6Ac 1.1 cm and Fig 6Ab 1 cm, Fig 6Bb 0.9 cm), whereas the pure P(C980-AM) hydrogels (Fig. 6A,Ba 0.0 cm) showed no inhibition ability. The dual inorganic nanoparticles that were formed, contain hydrogels that have two kinds of metallic surfaces and charges, and these dual inorganic nanoparticle nanohydrogels interact more effectively with bacteria in comparison to other nanohydrogels. Therefore, C980 in combination with core–shell nanocomposite hydrogels exhibits excellent antibacterial activity. Above all, the mechanism was further supported by the studies of Singh *et al.*, which postulated that nanoparticles formed in the range 1–10 nm attach to the surface of the cell membrane and drastically disturb its proper function by forming pits.[31] The core–shell nanoparticles formed using the present approach, were in the range of 2–8 nm, which strongly supports the proposed mechanism.

4. Conclusion

In conclusion, a highly effective green process for the fabrication of a novel bioactive core–shell nanocomposite hydrogel was developed with Carbopol® 980 NF as a stabilizing agent for the core–shell nanoparticles. The core–shell (Ag^0–Au^0) nanoparticles were prepared by reducing ($AgNO_3$ + $HAuCl_4$) inorganic salts with mint extract into the hydrogel network. These composites were developed and characterized by spectral, thermal and electron microscopy. The core–shell nanocomposite hydrogels prepared have significant antibacterial activity against *Bacillus* and *E. coli*. These results suggest that a core–shell nanoparticle containing hydrogels can be useful for effective and convenient treatment and inactivation of bacteria and may be helpful in developing effective pharmaceutical formulations for wound dressing by employing inorganic dual-metallic nanoparticles, loaded into the hydrogel networks.

Acknowledgements

Two of the authors (KVP & KRM) thank the Fondecyt Proyecto no: 3130748 & 1110583 UdeC, Chile (South America).

References

1 P. Ranga Reddy, K. Varaprasad, N. Narayana Reddy, K. Mohana Raju and N. Subbarami Reddy, *J. Appl. Polym. Sci.*, 2012, **125**, 829–1656.
2 K. Vimala, Y. Murali Mohan, K. Samba Sivudu, K. Varaprasad, S. Ravindra, N. Narayana Reddy, Y. Padma, B. Sreedhar and K. Mohana Raju, *Colloids Surf., B*, 2010, **76**, 248–258.
3 P. S. Keshava Murthy, Y. Murali Mohan, K. Varaprasad, B. Sreedhar and K. Mohana Raju, *J. Colloid Interface Sci.*, 2008, **318**, 217–224.
4 K. Varaprasad, Y. Murali Mohan, S. Ravindra, N. Narayana Reddy, K. Vimala, K. Monika, B. Sreedhar and K. MohanaRaju, *J. Appl. Polym. Sci.*, 2010, **115**, 1199–1207.
5 Y. Murali Mohan, K. Vimala, V. Thomas, K. Varaprasad, B. Sreedhar, S. K. Bajpai and K. Mohana Raju, *J. Colloid Interface Sci.*, 2010, **342**, 73–82.
6 K. Vimala, Y. M. Mohan, K. Varaprasad, N. N. Reddy, S. Ravindra, N. Sudhakar Naidu and K. Mohana Raju, *Int. J. Biomed. Nanosci. Nanotechnol.*, 2011, **2**, 55–64.
7 K. Varaprasad, Y. Murali Mohan, K. Vimala and K. Mohana Raju, *J. Appl. Polym. Sci.*, 2011, **121**, 784–796.
8 K. Varaprasad, N. Narayana Reddy, S. Ravindra, K. Vimala and K. Mohana Raju, *Int. J. Polym. Mater.*, 2011, **60**, 490–503.
9 K. Varaprasad, K. Vimala, S. Ravindra, N. Narayana Reddy, G. Venkata Subba Reddy and K. Mohana Raju, *J. Mater. Sci.: Mater. Med.*, 2011, **22**, 1863–1872.
10 K. Varaprasad, S. Ravindra, N. Narayana Reddy, K. Vimala and K. Mohana Raju, *J. Appl. Polym. Sci.*, 2010, **116**, 3593–3602.
11 K. Varaprasad, K. Vimala, S. Ravindra, N. Narayana Reddy and K. Mohana Raju, *Polym.-Plast. Technol. Eng.*, 2011, **50**, 1199–1207.
12 Y. Murali Mohan, T. Premkumar, K. Lee and K. E. Geckeler, Fabrication of Silver Nanoparticles in Hydrogel Networks, *Macromol. Rapid Commun.*, 2006, **27**, 1346–1354.
13 T. Jayaramudu, G. M. Raghavendra, K. Varaprasad, R. Sadiku and K. Mohana Raju, *Carbohydr. Polym.*, 2013, **92**, 2193–2200.
14 S. C. G. Leeuwenburgh, J. A. Jansen and A. G. Mikos, *J. Biomater. Sci., Polym. Ed.*, 2007, **18**, 1547–1564.
15 G. M. Raghavendra, T. Jayaramudu, K. Varaprasad, R. Sadiku, K. M. Raju and S. S. Ray, *Carbohydr. Polym.*, 2013, **93**, 553–560.
16 S. Ravindra, A. F. Mulaba-Bafubiandi, V. Rajinikanth, K. Varaprasad, N. N. Reddy and K. Mohana Raju, *J. Inorg. Organomet. Polym. Mater.*, 2012, **22**, 1254–1262.
17 K. Varaprasad, K. Vimala, S. Ravindra, N. Narayana Reddy and K. Mohana Raju, *J. Polym. Environ.*, 2012, **20**, 573–582.
18 V. Chawla and S. A. Saraf, Rheological studies on solid lipid nanoparticle based carbopol gels of aceclofenac, *Colloids Surf., B*, 2012, **92**, 293–298.
19 R. E. Haaland, T. E. Strickfaden, A. Holder, C. P. Pau, J. M. McNicholl, S. Chaikummao, W. Chonwattana and

C. E. Hart, *Antimicrob. Agents Chemother.*, 2012, **6**, 3592–3596.
20 G. Rathnam, N. Narayanan and R. Ilavarasan, *AAPS PharmSciTech*, 2008, **9**, 1078–1082.
21 R. Rupp, S. L. Rosenthal and L. R. Stanberry, *Int. J. Nanomed.*, 2007, **2**, 561–566.
22 B. Gwendolyn, The Wall Street Journal, July 30 2009.
23 R. Karousou, M. Balta, E. Hanlidou and S. Kokkini, *J. Ethnopharmacol.*, 2007, **109**, 248–257.
24 K. Varaprasad, N. Narayana Reddy, N. Mithil Kumar, K. Vimala, S. Ravindra and K. MohanaRaju, *Int. J. Polym. Mater.*, 2010, **59**, 981–993.
25 B. Manjula, K. Varaprasad, R. Sadiku and K. Mohana Raju, *Adv. Polym. Technol.*, 2013, **32**, 21340.
26 N. Luo, K. Varaprasad, K. Subba Reddy, A. Varada Rajulu and J. Zhang, *RSC Adv.*, 2012, **2**, 8483–8488.
27 S. Ravindra, A. F. Mulaba-Bafubiandi, V. Rajineekanth, K. Varaprasad and K. Mohana Raju, *Polym.-Plast. Technol. Eng.*, 2012, **51**, 1355–1360.
28 S. H. Park, M. K. Chun and H. K. Choi, *Int. J. Pharm.*, 2008, **347**, 39–44.
29 H. H. Lara, E. N. Garza-Treviño, L. Ixtepan-Turrent and K. S. Dinesh, *J. Nanobiotechnol.*, 2011, **9**, 30.
30 N. A. Amro, L. P. Kotra, K. Wadu-Mesthrige, A. Bulychev, S. Mobashery and G. Liu, *Langmuir*, 2000, **16**, 2789–2796.
31 M. Singh, S. Singh, S. Prasada and I. S. Gambhir, *J. Nanomater. Biostruct.*, 2008, **3**, 115–122.